Asia Pacific Academy of Science Pte. Ltd.

Mathematics and Systems Science 2024, 2(2), 2885.
https://doi.org/10.54517/mss2885

Article

Stability analysis of the SEIRS epidemic model with infectious dynamics during latent and infectious periods

Guichen Lu[1,2,*], Yifan Miao[1]

[1] School of Science, Chongqing University of Technology, Chongqing 400054, China

[2] School of Mathematics Sciences, University of Electronic Science and Technology of China, Chengdu 611731, China

*** Corresponding author:** Guichen Lu, guichenlu@cqut.edu.cn

CITATION

Lu G, Miao Y. Stability analysis of the SEIRS epidemic model with infectious dynamics during latent and infectious periods. Mathematics and Systems Science. 2024; 2(2): 2885. https://doi.org/10.54517/mss2885

ARTICLE INFO

Received: 15 August 2024
Accepted: 13 September 2024
Available online: 30 September 2024

Abstract: Coronary pneumonia caused by the SARS-CoV-2 virus was one of the most significant public health threats in recent years. In this paper, we develop and investigate an SEIRS epidemic model that incorporates infectivity during both the latent and infectious stages to characterize the transmission dynamics of COVID-19. By calculating the basic reproduction number (R_0) and applying monotonic dynamical system theory along with geometric methods, we validate the threshold theorem. Our analysis demonstrates that the disease-free equilibrium is globally stable when $R_0 < 1$, while the endemic equilibrium becomes globally stable when $R_0 > 1$.

Keywords: COVID-19; SEIRS epidemic model; Basic reproduction number; Global stability

1. Introduction

The COVID-19 pandemic, caused by the SARS-CoV-2 virus, has rapidly spread worldwide, leading to significant economic disruptions and a major public health crisis. For the purpose of responding to the epidemic and providing theoretical support for epidemic prevention and control, a number of researchers have committed themselves to numerical fitting of COVID-19 data in real-time as well as the risk assessment of COVID-19 prevalence. Based on the epidemiological and clinical characteristics of COVID-19, scholars usually employ the SEIR epidemiological model and its improved version to study the spread of COVID-19 [1–5]. The results of the above research not only explain how COVID-19 disease evolved over time, but also assess the risk of disease transmission.

Stability analysis is also a common technique used to study COVID-19 transmission. Annas et al.[2] developed the SEIR model with an effective vaccination rate and assessed vaccination's impact on COVID-19 epidemic patterns through the use of stability theory and numerical simulations. In [6], the researchers introduced a nonlinear coupled model to capture the dynamics of COVID-19 spread and assess the global stability of the disease-free equilibrium. Meanwhile, Abdulla et al. [7] developed a SHIQ model to illustrate the transmission dynamics of the virus and employed Lyapunov stability theory to analyze both the global and local stability of disease-free and endemic equilibria.

Considering the influence of age structure and other spatial factors, recent advancements in epidemic modeling emphasize the critical role of variable parameters and fractional derivatives. Al-Arydah [8] developed an SIRS model incorporating vaccination

and variable immunity durations, demonstrating that the basic reproduction number is highly sensitive to changes in immunity loss rates and that extending the vaccine's immunity period significantly enhances disease control effectiveness. Bouissa et al. [9] investigated the global dynamics of a time-fractional SIR model with reaction-diffusion equations, highlighting the impact of public health measures, such as mask-wearing, on disease transmission. Furthermore, Bouissa and Tsoul [10] conducted an in-depth analysis of disease dynamics by integrating the Crowley-Martin functional response and saturation treatment mechanisms into a nonlinear fractional-order SEIRS model. Their study revealed how changes in the fractional order and associated memory effects influenced the interactions among different compartments, shedding light on the local and global stability of the model's equilibria.

Taking into account the literature discussed above, the objective of this paper is to examine the trends in the evolution of COVID-19 using the SEIRS infectious disease model. Moreover, we will analyze the global stability of the model, which will help us determine the final evolution of the disease and demonstrate that the government's prevention and control measures are necessary to combat COVID-19. The structure of this paper is as follows: Section 2 provides a comprehensive description of the proposed mathematical model. Section 3 presents an in-depth analysis of the model's dynamic behavior. In Section 4, we summarize the key findings of the study, emphasizing important insights derived from numerical simulations.

2. Formation of the SEIRS epidemic model for COVID-19

When COVID-19 is present in a region, individuals initially fall into the susceptible category, with a significant portion eventually transitioning to the exposed state. After an approximate 14-day latent period, those who are exposed become infectious. They then recover, gaining temporary immunity, and subsequently return to the susceptible state. Furthermore, the transmission characteristics of COVID-19 indicate that individuals in both the latent and susceptible stages have the potential to spread the disease.

Considering the transmissibility of COVID-19 during both the incubation and infectious periods, and drawing on the work of Liu et al. [11], we utilize the incidence function $f(S, E, I) = \beta S^q(\theta E + I)$ as shown in Flowchart 1.

The parameter β indicates the transmission rate, reflecting how quickly susceptible individuals become infected through interactions with infected individuals. On the other hand, θ is a modification factor that adjusts the transmission rate for those who are in the exposed stage compared to those who are symptomatic. If θ is less than 1, it implies that individuals in the exposed stage have a lower likelihood of transmitting the disease compared to symptomatic individuals.

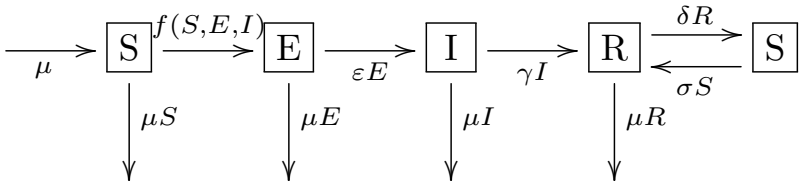

Figure 1. A sketch of the SEIRS transmission scheme for COVID-19.

Meanwhile, the parameter $q > 0$ typically represents an adjustment factor that modifies the influence of the susceptible population (S) on the transmission rate of the disease. When $q = 1$, the transmission rate is directly proportional to the number of susceptible individuals, indicating a linear relationship. If $q > 1$, it reflects a super-linear effect, meaning that as the number of susceptible individuals increases, the transmission rate rises more rapidly. On the other hand, $q < 1$, the effect is sub-linear, meaning that the impact of an increasing number of susceptible individuals on the transmission rate diminishes.

According to scheme in **Figure 1**, the COVID-19 model can be interpreted as follows:

$$\begin{cases} S' = \mu - (\mu + \sigma)S - \beta S^q(I + \theta E) + \delta R, \\ E' = \beta S^q(I + \theta E) - \mu E - \varepsilon E, \\ I' = \varepsilon E - \mu I - \gamma I, \\ R' = \sigma S + \gamma I - \mu R - \delta R \end{cases} \tag{1}$$

where $S(t)$, $E(t)$, $I(t)$, and $R(t)$ represent the proportions of individuals who are susceptible, exposed, infected, and recovered from the disease, respectively, at time t. Each of the parameters is described in detail in **Table 1**.

Table 1. Detailed explanation of the parameters for model (1).

Parameter	**Description**
β	Rate at which the disease spreads
μ	Proportion of natural births and deaths
ϵ	Rate of transition from exposed (E) to infected (I)
γ	Rate of recovery or transition from infected I to recovered (R)
δ	The rate at which recovered individuals become susceptible
σ	Vaccination rate of susceptible populations

For the purpose of preventing the spread of SARS-COV-2 virus, the government has implemented several strategies to curb the spread of epidemic viruses, including ordering citizens to wear facemasks, imposing travel restrictions, offering vaccinations, and requiring patients to stay at home or in hospitals. Once the measures have been taken, the transmission rates β will begin to decrease. To be reasonable, β must be a

function, and the model (1) could be written as

$$\begin{cases} S' = \mu - (\mu + \sigma)S - \beta(t)S^q(I + \theta E) + \delta R, \\ E' = \beta(t)S^q(I + \theta E) - \mu E - \varepsilon E, \\ I' = \varepsilon E - \mu I - \gamma I, \\ R' = \sigma S + \gamma I - \mu R - \delta R \end{cases} \tag{2}$$

Based on the work of Al-Arydah [12], in model (2), it is assumed that the transmission rate function $\beta(t)$ is a two-stage monotone decreasing function:

$$\beta(t) = \begin{cases} \beta_0 \exp(-m(t - t_l)) & t \geq t_l \\ \beta_0 & t < t_l \end{cases} \tag{3}$$

where t_l represents the time at which interventions to control the COVID-19 outbreak are implemented, and $m \geq 0$ denotes the rate of exponential decline, reflecting the intensity of the social restrictions.

Following a period of implementing prevention and control measures, once the COVID-19 outbreak is brought under control, the intensity of these measures may be eased. However, this relaxation could potentially result in a resurgence of the outbreak, as observed in Ukraine. In the case of two waves of COVID-19 outbreaks, we assume that the transmission rate function follows a four-stage model.

$$\beta(t) = \begin{cases} \beta_0 & t < t_l \\ \beta_0 \exp(-m_1(t - t_l)) & t_l \leq t < t_r \\ \beta_1 & t_r \leq t < t_L \\ \beta_1 \exp(-m_2(t - t_L)) & t \geq t_L \end{cases} \tag{4}$$

where t_r is the time for epidemic prevention and control to loosen up, while t_L is the time to start preventing and controlling epidemics again. $m_i > 0$ $(i = 1, 2)$ represents the exponential decay rate and quantifies the intensity of the social restrictions.

3. Analysis of the SEIRS model (1)

Due to the fact that $S + E + I + R = 1$, the biologically feasible region

$$\Omega = \{(S, E, I, R) \in R_+^4 \mid S + E + I + R \leq 1\} \tag{5}$$

Is positively invariant with respect to the system (1). Therefore, we focus on solutions originating in region Ω, where general existence, uniqueness, and continuation results are all valid.

3.1. Existence of equilibria and basic reproduction number

The objective of this section is to determine all steady states of the system and calculating its basic reproduction number. It is straightforward to determine that system

(1) always has an equilibrium free from disease

$$P_0 = (\frac{\delta+\mu}{\delta+\mu+\sigma}, 0, 0, \frac{\sigma}{\delta+\mu+\sigma})$$

Using the next-generation matrix approach, the basic reproduction number R_0 can be defined as:

$$R_0 = \rho(FV^{-1}) \tag{6}$$

Here, FV^{-1} represents the next-generation matrix, and ρ denotes the spectral radius of this matrix.

A simple calculation leads to

$$F = \begin{bmatrix} \beta\theta S_0^q & \beta S_0^q \\ 0 & 0 \end{bmatrix}, \; V = \begin{bmatrix} \varepsilon+\mu & 0 \\ -\varepsilon & \mu+\gamma \end{bmatrix} \tag{7}$$

with $S_0 = \dfrac{\delta+\mu}{\delta+\mu+\sigma}$.

Therefore, the basic reproduction number can be calculated as follows:

$$R_0 = \frac{\beta\, {S_0}^q(\varepsilon+\theta(\gamma+\mu))}{(\varepsilon+\mu)(\mu+\gamma)} \tag{8}$$

Additionally, the system features an endemic equilibrium that is determined by the basic reproduction number, which is defined as follows:

$$P^* = (S^*, E^*, I^*, R^*), \tag{9}$$

where $S^* = S_0 {R_0}^{-\frac{1}{q}}$, $E^* = \dfrac{(\mu+\gamma)}{\epsilon} I^*$, $R^* = \dfrac{\gamma I^* + \sigma\, S^*}{\delta+\mu}$ and

$$I^* = \frac{(\delta+\mu)\,\epsilon}{(\epsilon+\mu)\,(\mu+\gamma)+(\gamma+\epsilon+\mu)\,\delta}\left(1-(\frac{1}{R_0})^{\frac{1}{q}}\right)$$

Consequently, we have

Theorem 1. *The endemic equilibrium P^* of the model* (1) *can only exist if and only if $R_0 > 1$.*

3.2. Global Stability Analysis SEIRS model (1)

3.2.1. Global Stability Analysis of the Disease-Free Steady State

With the basic reproduction number R_0 in mind, we can arrive at the following conclusion:

Theorem 2. *If $R_0 < 1$, the disease-free equilibrium P_0 of the model* (1) *is both locally and globally asymptotically stable. Conversely, if $R_0 > 1$, it becomes unstable.*

Proof. At the disease-free equilibrium point P_0, the Jacobian matrix associated with

the model (1) is given by

$$J_{P_0} = \begin{bmatrix} -\mu-\sigma & -\beta\theta {S_0}^q & -\beta\, {S_0}^q & \delta \\ 0 & \beta\theta {S_0}^q - \epsilon - \mu & \beta\, {S_0}^q & 0 \\ 0 & \epsilon & -\gamma-\mu & 0 \\ \sigma & 0 & \gamma & -\delta-\mu \end{bmatrix} \tag{10}$$

The characteristic equation of matrix J_{P_0} can be expressed as follows:

$$(\lambda+\mu)\left(\lambda+\delta+\mu+\sigma\right)\left(\lambda^2+a_1\lambda+a_2\right)=0 \tag{11}$$

where $a_1=(-\beta\theta S_0+\epsilon+\gamma+2\mu)$ and $a_2=-(\epsilon+\mu)(\mu+\gamma)(R_0-1)$. Equation (11) gives four characteristic roots. They are

$$\lambda_1=-\mu, \lambda_2=-(\delta+\mu+\sigma)$$

and λ_3, λ_4. satisfy

$$\lambda_3+\lambda_4=-a_1, \lambda_3\lambda_4=a_2$$

From (8), we observe that

$$R_0=\frac{\beta\varepsilon {S_0}^q}{(\varepsilon+\mu)(\mu+\gamma)}+\frac{\beta\theta {S_0}^q}{\varepsilon+\mu}>\frac{\beta\theta {S_0}^q}{\varepsilon+\mu}$$

It follows that if $R_0<1$ there will be $a_1>0, a_2>0$, which implies that the real parts of all four eigenvalues of J_{p_0} are negative. If $R_0>1$, then λ_1 and λ_2 are negative and one of λ_3, λ_4 will have a positive real part. To summarize, P_0 is locally asymptotically stable when P_0 and becomes unstable when P_0.

Put $R=1-S-E-I$ into the first equation of the model (1), we get

$$S' \leq (\mu+\delta)-(\mu+\sigma+\delta)S$$

By integrating the previous differential inequality, the following result is obtained

$$0 \leq S(t) \leq S_0-(S_0-S(0))\mathrm{e}^{-(\delta+\mu+\sigma)t}$$

When $t\to\infty$, we have $0\leq S(t)\leq S_0$, and there exists a time $T>0$ such that for $t>T$,

$$0\leq S(t)\leq S_0$$

Based on the second and third equations of model (1), it can be deduced that

$$\begin{cases} E' \leq (\beta\theta S_0^q-\varepsilon-\mu)E+\beta S_0^q I, \\ I'=\varepsilon E-(\gamma+\mu)I \end{cases} \tag{12}$$

Let's look at the differential equations below

$$\begin{cases} \bar{E}' = (\beta\theta S_0^q - \varepsilon - \mu)\bar{E} + \beta S_0^q \bar{I}, \\ \bar{I}' = \varepsilon\bar{E} - (\gamma + \mu)\bar{I} \end{cases} \tag{13}$$

Based on (7), (13) has the following matrix form.

$$Y' = (F - V)Y \tag{14}$$

where $Y = (\bar{E}, \bar{I})^T$.

It can be seen that the global stability of the linear Equation (15) is determined by the stability of the matrix $F - V$. Lemma 2 in [13] shows that, if $R_0 < 1$, then

$$s(F - V) < 0$$

with s being the maximum real part of each eigenvalue accordingly. Therefore, all the solutions in (15) satisfy

$$\lim_{t\to\infty} \bar{I}(t) = 0, \lim_{t\to\infty} \bar{E}(t) = 0 \tag{15}$$

we can conclude from the comparison principle that each solution of (13) satisfies

$$\lim_{t\to\infty} I(t) = 0, \lim_{t\to\infty} E(t) = 0 \tag{16}$$

Consequently, (1) has a limiting system

$$\begin{cases} S' = \mu - (\mu + \sigma)S + \delta R, \\ R' = \sigma S - (\delta + \mu)R \end{cases} \tag{17}$$

The Jacobian matrix of system (17) is a Metzler matrix, thus, it can be concluded that system (3.14) is a cooperative system with a unique equilibrium

$$\tilde{P}_0 = (\frac{\delta + \mu}{\delta + \mu + \sigma}, \frac{\sigma}{\delta + \mu + \sigma}).$$

Using the monotone system theory developed in [14], We propose that $\tilde{P}_0$ of system (17) is globally asymptotically stable.

In terms of limit system theory [15], the unique positive equilibrium P_0 is a global attractor of model (1). Since (1) is local asymptotic stability, this implies that it is global asymptotic stability. We have now proved the Theorem. □

3.3. Global stability of the endemic equilibrium

3.3.1. Liu-Hethcote-Levin conjecture

If $\sigma = \theta = 0$, system (1) is the Liu-Hethcote-Levin's model. The following conjecture was put forward by them in [11].

Conjecture 1. ***(Liu-Hethcote-Levin conjecture.)*** *Suppose $R_0 > 1$, then the endemic*

equilibrium of the system (1) *is globally asymptotically stable if* $\sigma = \theta = 0$.

It has been extensively studied in literature since the Liu-Hethcote-Levin conjecture was formulated. According to Li-Muldowney's geometric approach, partial answers can be obtained in [16–19], while complete answers are given by Lu and Lu in [20].

With $\theta > 0$ and $\sigma = 0$, the model (1) is a SEIRS epidemic model with infectious force in the latent and infected periods. By building a proper Lyapunov function and using Lyapunov's direct method, Jiao, Liu and Cai [3] have obtained a sharp threshold condition of global asymptotic stability when $\delta = 0$. Additionally, Li and her colleagues' results [21,22] suggest some conditions that are sufficient for global stability.

As a natural question, one might wonder whether the dynamic behavior of the SEIRS infectious disease model (2.1) match that of the Liu-Hethcote-Levin conjecture when $\sigma > 0$ and $\theta > 0$.

Problem 1. *Is the Liu-Hethcote-Levin conjecture valid if* $\theta > 0$ *and* $\sigma > 0$ *?*

Theorem 4.3 from [19] offers a clear and practical implication: if the disease-free equilibrium P_0 is unstable, then the system exhibits uniform persistence. Thus the following conclusion can be proved in the same manner as in the proof of proposition 3.3 in [23].

Proposition 1. *Model* (1) *is uniformly persistent in* Ω *if* $R_0 > 1$.

3.3.2. Geometric criterion for global stability

Consider a system of differential equations with an invariant $n - r$ dimensional manifold:

$$\dot{x} = f(x) \tag{18}$$

Let D be a subset of $\mathbb{R}^n$. The invariant manifold Γ is defined as the set of all points x in D that satisfy $h(x) = 0$, i.e.,

$$\Gamma = \{x \in D \subset R^n \mid h(x) = 0\} \tag{19}$$

where $h(x)$ is a continuously differentiable function defined on D, and the rank of the Jacobian matrix $\frac{\partial h}{\partial x}$ is r when $h(x) = 0$.

Drawing upon the geometric techniques developed by Li and Muldowney [18,24], Lu and Lu [20] have proposed a new criterion for determining global stability.

Theorem 3. ([20])

Assume that the system (18) *meets the following conditions:*

($\mathbf{H_1}$) *The simply connected set* Γ *contains a compact absorbing subset* K.

($\mathbf{H_2}$) *There is a unique equilibrium* $\bar{x} \in K \subset \Gamma$ *in system* (18)*;*

($\mathbf{H_3}$) *There exist* $\tilde{g}_i(t)$ *and some positive numbers* κ_i, $i \in N = \{1, 2, \cdots, n\}$ *such*

that for all $t \geq T$ *and for all* $x_0 \in K$,

$$\tilde{b}_{ii}(t) + \sum_{i \neq j} \frac{\kappa_j}{\kappa_i} |\tilde{b}_{ij}(t)| \leq \tilde{g}_i(t) \text{ with } \lim_{t \to +\infty} \frac{1}{t} \int_0^t \tilde{g}_i(t) = \tilde{\delta}_i < 0$$

where $\tilde{b}_{ij}(t)$ *represent the elements of coefficient matrix*

$$\tilde{B}(t) = \tilde{B}(x(t)) = \dot{P}_f P^{-1} + P \frac{\partial f^{[r+2]}}{\partial x}(x(t, x_0)) P^{-1} - \nu(x) I \tag{20}$$

Here $\nu(x)$ *and* $P(x)$ *are defined as in* [20,24]. *Then the unique equilibrium* $\bar{x}$ *of* (18) *is globally stable in* Γ.

3.3.3. Global analysis of model

If $\sigma = 0, \theta = 1$, model (1) can be written as

$$\begin{cases} S' = \mu - \mu S - \beta S^q (I + E) + \delta R, \\ E' = \beta S^q (I + E) - (\varepsilon + \mu) E, \\ I' = \varepsilon E - (\gamma + \mu) I, \\ R' = \gamma I - (\delta + \mu) R \end{cases} \tag{21}$$

Our main result is as follows.

Theorem 4. *If* $\sigma = 0, \theta = 1$ *and* $R_0 > 1$, *the epidemic equilibrium* P^* *of model* (21) *is globally asymptotically stable in* Γ.

Proof. Let $x = (S, E, I, R) \in R_+^4$, and $h(x) = S + E + I + R - 1$, from Proposition 3.1 in [24], it is easy to deduce that

$$\Sigma = \{x \in R_+^4 \mid h(x) = 0\}$$

is a three dimensional invariant manifold with $\nu(x) = -\mu$ and $m = \dim \frac{\partial h}{\partial x} = 1$.

From the invariance of Σ and Proposition 1, it follows that there exist a large enough $T > 0$ and a constant $m_0 > 0$, such that for each $t > T$,

$$m_0 \leq S, E, I, R \leq 1 \tag{22}$$

which implies the existence of a compact set $K \subset \Sigma$.

Our next task is to check condition (H_3) in Theorem 3 hold, we will divide it into two cases.

Case 1: If $\gamma \geq \varepsilon$.

An easy computation shows that the Jacobian matrix $J(x) = \frac{\partial f}{\partial x}$ of system (21)

can be expressed as follows:

$$J(x)=\begin{bmatrix} -\beta qS^{q-1}(I+E)-\mu & -\beta S^q & -\beta S^q & \delta \\ \beta qS^{q-1}(I+E) & \beta S^q-\varepsilon-\mu & \beta S^q & 0 \\ 0 & \varepsilon & -\gamma-\mu & 0 \\ 0 & 0 & \gamma & -\delta-\mu \end{bmatrix}$$

According to the definition of the third additive compound matrix, $J^{[3]}(x)$ is given by the following expression:

$$J^{[3]}(x)=\begin{bmatrix} -\varepsilon-\gamma & 0 & 0 & \delta \\ \gamma & -\varepsilon-\delta & \beta S^q & \beta S^q \\ 0 & \varepsilon & -\gamma-\delta & -\beta S^q \\ 0 & 0 & \beta qS^{q-1}(I+E) & -\varepsilon-\gamma-\delta \end{bmatrix}+\Psi$$

Here $\Psi=\text{diag}\{\psi+\beta S^q,\psi+\beta S^q,\psi,\beta S^q-3\mu\}$ with $\psi=-\beta qS^{q-1}(I+E)-3\mu$.

Let $P(x)$ be defined by $P(x)=\text{diag}\{R,I,E,\frac{S}{q}\}$. An easy computation shows that

$$\begin{aligned}\tilde{B}(t)&=P_fP^{-1}+P\frac{\partial f}{\partial x}^{[3]}P^{-1}-\nu I_{4\times 4}\\&=\begin{bmatrix} -\varepsilon-\gamma & 0 & 0 & \delta q\frac{R}{S} \\ \frac{\gamma I}{R} & -\varepsilon-\delta & \frac{\beta S^qI}{E} & \beta qS^{q-1}I \\ 0 & \frac{\varepsilon E}{I} & -\gamma-\delta & -\beta qS^{q-1}E \\ 0 & 0 & \beta\frac{S^q(I+E)}{E} & -\varepsilon-\gamma-\delta \end{bmatrix}+\Phi\end{aligned} \tag{23}$$

where $\Phi=\text{diag}\{\psi+\beta S^q+\mu+\frac{R'}{R},\psi+\beta S^q+\mu+\frac{E'}{E},\psi+\mu+\frac{I'}{I},\beta S^q-2\mu+\frac{S'}{S}\}$.

Rewrite the system of equations as follows

$$\begin{aligned}&\frac{\varepsilon E}{I}=\frac{I'}{I}+\gamma+\mu,\frac{\gamma I}{R}=\frac{R'}{R}+\delta+\mu,\frac{\beta S^q(I+E)}{E}=\frac{E'}{E}+\varepsilon+\mu,\\&\frac{\delta R}{S}=\beta S^{q-1}(I+E)+\mu(1-\frac{1}{S})+\frac{S'}{S}\end{aligned}$$

From (22), we can can deduce that there exists an $\underline{m}>0$, such that

$$\beta qS^{q-1}E\le\beta q\underline{m}_0{}^q\triangleq\underline{m}>0$$

Consequently,

$$\begin{aligned} h_1(t) &= b_{11}(t) + \sum_{j=2}^{4} |b_{1j}(t)| \\ &= -\beta q S^{q-1}(I+E) + \beta S^q - 2\mu - \varepsilon - \gamma + \frac{R'}{R} + \delta q \frac{R}{S} \\ &= \beta S^q - 2\mu - \varepsilon - \gamma + \frac{R'}{R} + q\mu(1 - \frac{1}{S}) + q\frac{S'}{S} \end{aligned}$$

$$\begin{aligned} &= -\frac{\beta S^q I}{E} - 2\mu - \varepsilon - \gamma + \varepsilon + \mu + \frac{R'}{R} + q\mu(1 - \frac{1}{S}) + q\frac{S'}{S} + \frac{E'}{E} \\ &= -\frac{\beta S^q I}{E} - \mu - \gamma + \frac{R'}{R} + \mu q(1 - \frac{1}{S}) + q\frac{S'}{S} + \frac{E'}{E} \\ &\leq -\mu - \gamma + \frac{R'}{R} + q\frac{S'}{S} + \frac{E'}{E} \end{aligned}$$

and

$$\begin{aligned} h_2(t) &= b_{22}(t) + \sum_{i \neq j} |b_{2j}(t)| \\ &= -\beta q S^{q-1}(I+E) + \beta S^q + \frac{\beta S^q I}{E} + \beta q S^{q-1} I - 2\mu - \varepsilon - \delta + \frac{E'}{E} + \frac{\gamma I}{R} \\ &= -\beta q S^{q-1} E + 2\frac{E'}{E} + \frac{R'}{R} \leq -\underline{m} + 2\frac{E'}{E} + \frac{R'}{R} \end{aligned}$$

Similarly,

$$\begin{aligned} h_3(t) &= b_{33}(t) + \sum_{i \neq j} |b_{3j}(t)| \\ &= -\beta q S^{q-1}(I+E) - 2\mu - \gamma - \delta + \beta q S^{q-1} E + \frac{I'}{I} + \frac{\varepsilon E}{I} \\ &= -\beta q S^{q-1} I - 2\mu - \gamma - \delta + 2\frac{I'}{I} + (\gamma + \mu) \\ &= -\beta q S^{q-1} I - \mu - \delta + 2\frac{I'}{I} \\ &\leq -\mu - \delta + 2\frac{I'}{I} \end{aligned}$$

and

$$\begin{aligned} h_4(t) &= b_{44}(t) + \sum_{i \neq j} |b_{4j}(t)| \\ &= -2\mu - \gamma - \delta - \varepsilon + \frac{S'}{S} + \beta\frac{S^q(I+E)}{E} + \beta S^q \\ &= -2\mu - \gamma - \delta - \varepsilon + \frac{S'}{S} + 2\beta\frac{S^q(I+E)}{E} - \beta\frac{S^q I}{E} \\ &\leq -2\mu - \gamma - \delta - \varepsilon + \frac{S'}{S} + 2(\varepsilon + \mu + \frac{E'}{E}) \\ &\leq -\gamma - \delta + \varepsilon + \frac{S'}{S} + 2\frac{E'}{E} \end{aligned}$$

Define functions $\tilde{g}_i(t)$ of condition (H_3) by

$$\tilde{g}_1(t) = -\mu - \gamma + \frac{R'}{R} + q\frac{S'}{S} + \frac{E'}{E},\ \tilde{g}_2(t) = -\underline{m} + 2\frac{E'}{E} + \frac{R'}{R}$$

and

$$\tilde{g}_3(t) = -\mu - \delta + 2\frac{I'}{I},\ \tilde{g}_4(t) = -\gamma - \delta + \varepsilon + \frac{S'}{S} + 2\frac{E'}{E}$$

By virtue of condition (22), we get

$$\lim_{t\to+\infty} \frac{1}{t}\int_0^t \tilde{g}_i(t) = \bar{h}_i < 0 \tag{24}$$

where $\bar{h}_1 = -\mu - \gamma, \bar{h}_2 = -\underline{m}, \bar{h}_3 = -\mu - \delta, \bar{h}_4 = \varepsilon - \gamma - \delta$.

Case 2: If $\gamma < \varepsilon$.

We introduce transformation

$$s = S, e = E + (1 - \frac{\gamma}{\varepsilon})I, i = \frac{\gamma}{\varepsilon}I, r = R$$

but for simplicity of notation, we continue to use S, E, I, R for s, e, i, r.

Model (1) becomes

$$\begin{cases} S' = -\beta S^q(I+E) + \mu - \mu S + \delta R, \\ E' = \beta S^q(I+E) - (\gamma+\mu)E, \\ I' = \gamma E - (\varepsilon+\mu)I, \\ R' = \varepsilon I - (\delta+\mu)R \end{cases} \tag{25}$$

We shall adopt the same procedure as in the proof of **Case 1**, one can obtain that

$$\begin{aligned} \tilde{B}(t) &= P_f P^{-1} + P\frac{\partial f}{\partial x}^{[3]} P^{-1} - \nu I_{4\times 4} \\ &= \begin{bmatrix} -\varepsilon-\gamma & 0 & 0 & \delta q\frac{R}{S} \\ \frac{\varepsilon I}{R} & -\gamma-\delta & \frac{\beta S^q I}{E} & \beta q S^{q-1} I \\ 0 & \frac{\gamma E}{I} & -\varepsilon-\delta & -\beta q S^{q-1} E \\ 0 & 0 & \frac{\beta S^q(I+E)}{E} & -\varepsilon-\gamma-\delta \end{bmatrix} + \Phi \end{aligned} \tag{26}$$

where Φ is defined as in (23)

Similarly, we take functions $\tilde{g}_i(t)$ of condition (H_3) in Theorem 3 by

$$\begin{aligned} &\tilde{g}_1(t) = -\mu - \varepsilon + \frac{R'}{R} + q\frac{S'}{S} + \frac{E'}{E},\ \tilde{g}_2(t) = -\underline{m} + 2\frac{E'}{E} + \frac{R'}{R}, \\ &\tilde{g}_3(t) = -\mu - \delta + 2\frac{I'}{I},\ \tilde{g}_4(t) = \gamma - \delta - \varepsilon + \frac{S'}{S} + 2\frac{E'}{E} \end{aligned}$$

We conclude from condition (22) that

$$\lim_{t\to+\infty} \frac{1}{t}\int_0^t \tilde{g}_i(s)ds = \bar{h}_i < 0 \tag{27}$$

where $\bar{h}_1 = -\mu - \gamma, \bar{h}_2 = -\underline{m}, \bar{h}_3 = -\mu - \delta, \bar{h}_4 = \gamma - \delta - \varepsilon$.

From **Case 1** and **Case 2**, it follows that conditions (H_1)–(H_3) in Theorem 3 hold true, this establishes that the endemic equilibrium P^* possesses global asymptotic stability, thereby completing the proof.

4. Concluding remarks

In this study, we have developed and analyzed SEIRS epidemic models with infectious force in latent and infected periods to investigate the spread of COVID-19. Based on model (1), one can obtain the basic reproduction number as follows:

$$R_0 = \frac{\beta S_0^q \left(\varepsilon + \theta(\gamma + \mu)\right)}{(\varepsilon + \mu)(\mu + \gamma)}$$

With the help of monotonic dynamic systems theory and geometric methods, we have demonstrated that the disease-free equilibrium point of model (1) is locally and globally stable if and only if and only if $R_0 < 1$.

Based on the Lu-Lu stability theorem presented in [20], we can further conclude that when the basic reproduction number $R_0 > 1$, the positive equilibrium point of system (1) not only exists but also demonstrates global asymptotic stability. This implies that when $R_0 > 1$, the system will eventually reach stability, with all solutions converging to the positive equilibrium point. In epidemiological models, this finding is crucial as it indicates that once the disease's transmission potential exceeds a certain threshold, the proportion of infected individuals will stabilize, thus validating the model's effectiveness in describing the temporal dynamics of disease spread.

Table 2. Initial values of model (1) with $\theta = 1$ and $\sigma = 0$.

Variable	**value**	**Variable**	**value**
$S(0)$	0.99934957	$E(0)$	0.00039730
$I(0)$	0.00021936	$R(0)$	0.00003377

Table 3. Parameter value of model (2).

Variable	**value**	**Variable**	**value**	**Variable**	**value**
μ	0.0262	β	0.0571	ε	0.0257
γ	0.0476	q	0.9252	δ	0.1290

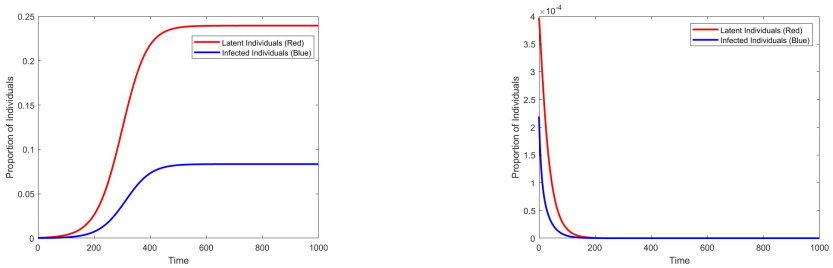

(a) $R_0 \approx 1.4867 > 1$ **(b)** $R_0 \approx 0.649 < 1$

Figure 2. Time Evolution of Infected Individual.

To demonstrate our findings, we give a numerical simulation. For the system

described by Equation (21), the parameter settings and initial values are detailed in **Tables 2** and **3**. Through numerical simulations, we observed (as shown in **Figure 2a**) that when the basic reproduction number $R_0 \approx 1.4867 > 1$ exceeds 1, the proportion of individuals in the latent and infected states tends to stabilize over time. This observation aligns with the conclusion of Theorem 4, indicating that the systems positive equilibrium point exhibits global stability.If we replace the parameter $\mu = 0.0262$ in **Table 3** with $\mu = 0.08$, resulting in $R_0 \approx 0.649 < 1$, the numerical simulation shows that over time, the number of latent and infected individuals eventually approaches zero (**Figure 2b**). This supports the conclusion of Theorem 2.

Although we have thoroughly examined the system's stability from a qualitative perspective, we have not yet conducted an in-depth analysis of the specific effects of the transmission rate function. Considering that some countries have experienced two waves of COVID-19, we model the transmission rate function using a four-stage function. Based on the initial values and model parameters provided in **Tables 2** and **4**, our graphical analysis reveals that the number of infected individuals exhibited two peaks over time before gradually declining to zero (**Figure 3**). This pattern is frequently observed in real-world pandemics, such as the similar fluctuations seen in Ukraine's COVID-19 outbreak in 2020.

Table 4. Parameter value of four-stage SEIRS model (2)

Variable	value	Variable	value	Variable	value
μ	0.0664	β_1	0.1024	ε	0.0183
γ	0.0275	q	0.0001	θ	0.4901
δ	0.005	m_2	0.0340	m_1	0.0095
t_l	220.1187	t_r	309.4841	t_L	364.0042
β	0.0972	σ	0		

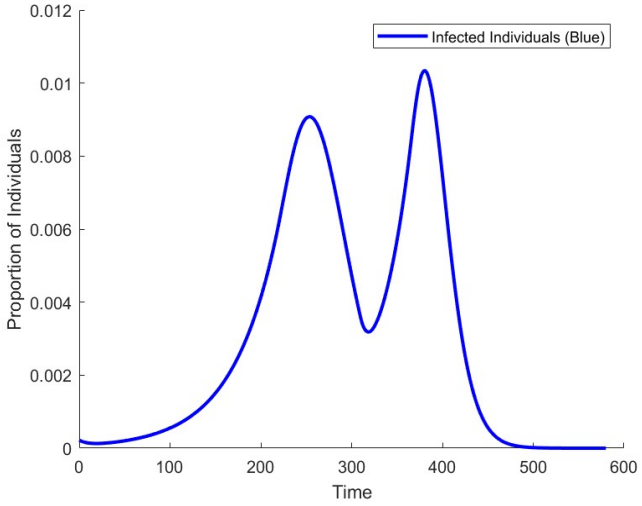

Figure 3. Time Evolution of Infected Individual.

The appearance of such fluctuations is likely influenced by multiple factors, including changes in public health policies, variations in public behavior, and virus mutations. However, we have not yet explored these fluctuations from a qualitative analytical per-

spective. To better understand this phenomenon, we plan to conduct further qualitative analyses to investigate the underlying causes and mechanisms behind these fluctuations. This research will enhance our understanding of how the transmission rate function affects epidemic dynamics and provide scientific insights for developing more effective pandemic control strategies.

Author contributions: Conceptualization, GL and YM; methodology, GL; software, GL and YM; validation, GL and YM; formal analysis, GL and YM; investigation, GL; resources, GL and YM; data curation, GL and YM; writing—original draft preparation, GL; writing—review and editing, GL and YM; visualization, YM; supervision, GL; project administration, GL; funding acquisition, GL. All authors have read and agreed to the published version of the manuscript.

Acknowledgments: Authors are thankful to editor and reviewers for their valuable comments and suggestion in the overall improvement of this article.

Funding: This research was partially supported by the Scientific and Technological Research Program of Chongqing Municipal Education Commission(Grant No. KJQN20180113). Additionally, it was funded by the Research Fund for the China Postdoctoral Science Foundation (Grant No. 2020M673166).

Conflict of interest: The authors declare no conflict of interest.

References

1. Alrashed S, Min-Allah N, Saxena A, et al. Impact of Lockdowns on the Spread of COVID-19 in Saudi Arabia. Informatics in Medicine Unlocked. 2020; 20: 100420.
2. Annas S, Pratama MI, Rifandi M, et al. Stability analysis and numerical aimulation of SEIR Model for pandemic COVID-19 spread in Indonesia. Chaos, Solitons and Fractals. 2020; 139: 110072.
3. Jiao J, Liu Z, Cai S. Dynamics of an SEIR model with infectivity in incubation period and homestead-isolation on the susceptible. Applied Mathematics Letters. 2020; 107: 106442.
4. Kyrychko YN, Blyuss KB, Brovchenko I. Mathematical modelling of the dynamics and containment of COVID-19 in Ukraine. Sci Rep. 2020; 10: 19662 .
5. Zu J, Li ML, Li ZF, et al. Transmission patterns of COVID-19 in the mainland of China and the efficacy of different control strategies: A data- and model-driven study. Infect Dis Poverty. 2020; 9: 83.
6. Zamir M, Shah K, Nadeem F, et al. Threshold Conditions for Global Stability of Disease Free State of COVID-19. Results in Physics. 2021; 21: 103784.
7. Abdullah, Ahmad S, Owyed S, et al. Mathematical analysis of COVID-19 via new mathematical model. Chaos, Solitons Fractals, Chaos, Solitons and Fractals. 2021; 143: 110585.
8. Al-arydah M. Assessing vaccine efficacy for infectious diseases with variable immunity using a mathematical model. Sci Rep. 2024; 14: 18572.
9. Bouissa A, Tahiri M, Tsouli N, et al. Global dynamics of a time-fractional spatio-temporal SIR model with a generalized incidence rate. J. Appl. Math. Comput. 2023; 69: 4779–4804.
10. Bouissa A and Tsouli N. Comprehensive analysis of disease dynamics using nonlinear fractional order SEIRS model with Crowley-Martin functional response and saturated treatment. International Journal of Biomathematics. 2024; 2350114.
11. Liu W, Hethcote HW, Levin SA. Dynamical behavior of epidemiological models with nonlinear incidence rates. J. Math. Biol. 1987; 25: 359–380.
12. Al-arydah M, Berhe H, Dib K, Madhu K. Mathematical modeling of the spread of the coronavirus under strict social restrictions. Math Meth Appl Sci. 2021; 1–11.
13. Van den Driessche P and Watmough J. Reproduction numbers and sub-threshold endemic equilibria for compartmental

models of disease transmission. Mathematical biosciences. 2002; 180: 29–48.
14. Jiang J. On the Global Stability of Cooperative Systems. Bulletin of the London Mathematical Society. 1994; 5: 455–458.
15. Thieme HR. Convergence results and a Poincar-Bendixson trichotomy for asymptotically autonomous differential equations. J. Math. Biol. 1992; 30: 755–C763.
16. Cheng Y and Yang X. On the global stability of SEIRS models in epidemiology. Can. Appl. Math. Q. 2012; 20: 115–133.
17. Li M, Muldowney JS. Global stability for the SEIR model in epidemiology. Math. Biosci. 1995; 125: 155–164.
18. Li M, Muldowney JS. A Geometric Approach to Global-Stability Problems. SIAM J. Math. Anal. 1996; 27: 1070–1083.
19. Li M, Muldowney JS, van den Driessche P. Global stability of SEIRS models in epidemiology. Can. Appl. Math. Q. 1999; 7: 409–425.
20. Lu G and Lu Z. Geometric approach to global asymptotic stability for the SEIRS models in epidemiology. Nonl. Anal. RWA. 2017; 36: 20–43.
21. Li G, Jin Z. Global stability of a SEIR epidemic model with infectious force in latent, infected and immune period. Chaos, Solitons and Fractals. 2005; 25: 1177–1184.
22. Li G, Wang W, Jin Z. Global stability of an SEIR epidemic model with constant immigration. Chaos, Solitons and Fractals. 2006; 30: 1012–1019.
23. Li M, Graef JR, Wang L, Karsai, J. Global dynamics of a SEIR model with varying total population size. Mathematical biosciences. 1999; 160: 191–213.
24. Li M, Muldowney JS. Dynamics of differential equations on invariant manifolds. J. Differential Equations. 2000; 168: 295–320.